International Journal of Heat and Mass Transfer 52 (2009) 466–472

Contents lists available at ScienceDirect

International Journal of Heat and Mass Transfer

journal homepage: www.elsevier.com/locate/ijhmt

Forced convective heat transfer of nanofluids in microchannels

Jung-Yeul Jung, Hoo-Suk Oh, Ho-Young Kwak *

Mechanical Engineering Department, Chung-Ang University, 221 Huksuk-Dong, Dongjak-Ku, Seoul 156-756, Republic of Korea

ARTICLE INFO

Article history:
Received 7 March 2007
Received in revised form 6 February 2008
Available online 22 July 2008

Keywords:
Convective heat transfer
Friction factor
Microchannel
Nanofluids

ABSTRACT

Convective heat transfer coefficient and friction factor of nanofluids in rectangular microchannels were measured. An integrated microsystem consisting of a single microchannel on one side, and two localized heaters and five polysilicon temperature sensors along the channel on the other side were fabricated. Aluminum dioxide (Al_2O_3) with diameter of 170 nm nanofluids with various particle volume fractions were used in experiments to investigate the effect of the volume fraction of the nanoparticles to the convective heat transfer and fluid flow in microchannels. The convective heat transfer coefficient of the Al_2O_3 nanofluid in laminar flow regime was measured to be increased up to 32% compared to the distilled water at a volume fraction of 1.8 volume percent without major friction loss. The Nusselt number measured increases with increasing the Reynolds number in laminar flow regime. The measured Nusselt number which turned out to be less than 0.5 was successfully correlated with Reynolds number and Prandtl number based on the thermal conductivity of nanofluids.

1. Introduction

Convective heat transfer in microchannel has been proved to be a very effective method for the thermal control micro electronic device [1–4]. In fact, a considerable heat flux of the order of 10^7 W/m^2 can be removed in microchannels with a surface temperature below 71 °C [1]. Another approach to enhance the convective heat transfer coefficient in the microchannel may be utilizing nanofluids as working fluids. This can be possible because the nanofluids having unprecedented stability of suspended nanoparticles were proven to be having anomalous thermal conductivity even with small volume fraction of the nanoparticles [5–7].

Various models have been proposed for explaining the mechanism of thermal conductivity enhancement with increasing temperature and decreasing nanoparticle sizes [8–11]. Through an order-of-magnitude analysis, Prasher et al. [12,13] have proposed that the localized convection due to the Brownian motion of nanoparticles is a key mechanism for the enhancement of the thermal conductivity of nanofluids. Further, the relationship between Brownian motion and enhanced thermal conductivity of nanoparticles was observed by optical visualization of the particles and measurement of the thermal conductivity [14].

Less extensive study on the measurement of the convective heat transfer coefficient with nanofluids has been done. Pak and Cho [15] measured the convective heat transfer coefficient with nanoparticles of γ-Al_2O_3 and TiO_2 dispersed in water. Their experimental results have revealed that the heat transfer coefficients of the nanofluids increase with increasing the volume fraction of nanoparticles and the Reynolds number. Their heat transfer data showed Nusselt numbers up to 30% higher than predicted by the pure liquid correlation. Lee and Choi [16] have found that the nanofluid in the microchannel heat exchanger dramatically enhances cooling rate compared with the conventional water cooled and liquid-nitrogen-cooled microchannel heat exchangers. Xuan and Li [17] measured the convective heat transfer coefficient and friction factor of Cu–water nanofluids of the turbulent flow in a brass tube of the inner diameter of 10 mm. Their experimental results have shown that the nanofluid enhances remarkably the heat transfer coefficients without substantial increase in the friction factor. A correlation for the convective heat transfer coefficient of nanofluid was also suggested by considering the microconvection and microdiffusion of the suspended nanoparticles. Convective heat transfer coefficients of nanofluids, made of γ-Al_2O_3 nanoparticles in deionized water along a copper tube of 4.5 mm diameter in laminar flow regime were measured by Wen and Ding [18]. They obtained significant enhancement in the entrance region and some decrease along the axial direction to approach a constant value. Recently, Buongiorno [19] suggested that a reduction of viscosity within and consequent thinning of the laminar sublayer leads to abnormal increase in the convective heat transfer coefficient in turbulent flow regime.

In this study, convective heat transfer coefficient and friction factor of Al_2O_3 nanofluids in rectangular microchannels were measured in laminar flow regime. The measured Nusselt number which turned out to be less than 0.5 was successfully correlated to the Reynolds number and Prandtl number based on the thermal conductivity of nanofluids.

* Corresponding author. Tel.: +82 2 820 5278; fax: +82 2 826 7464.
E-mail address: kwakhy@cau.ac.kr (H.-Y. Kwak).

0017-9310/$ - see front matter © 2008 Elsevier Ltd. All rights reserved.
doi:10.1016/j.ijheatmasstransfer.2008.03.033

Nomenclature

A	area
C	constant
C_p	specific heat of liquid
D_h	hydraulic diameter
f	friction factor
h	heat transfer coefficient
k_N	thermal conductivity of nanofluids
L	channel length
Nu	Nusselt number
P	Perimeter
Pr	Prandtl number
Re	Reynolds number
T	temperature
x	distance from channel inlet
Subscripts	
ch	channel
res	reservoir
f	fluid
in	inlet
w	wall
Greek letters	
ϕ	volume fraction of nanoparticle

2. Device design and fabrication

A silicon wafer polished on both sides (p-type ⟨100⟩ single crystal with 525 μm (±5μm) thickness) was used to fabricate an integrated microsystem consisting of a single channel on one side and two localized heaters and five polysilicon temperature sensors along the channel on the other side. A 17 mm × 33 mm die for the device was used. The fabrication of the device began with the thermal growth of a 0.5 μm oxide layer on the front side of the silicon wafer. A 0.540 μm polysilicon film was deposited on the top of the oxide layer and patterned to serve as the heater and temperature sensors. The length of the temperature sensors was fabricated to be the same as the width of the flow channel. The silicon temperature sensors having width of 10 μm were found to have a good current-resistance characteristics [20,21] so that one can measure the temperature of the channel wall in contact with the sensors. On the back side of the wafer, an oxide layer was also formed and patterned to serve as an etch mask for plasma etching, which produced a 50 μm or 100 μm deep flow channel with rectangular cross section. The microchannel was etched by using Bosch process with the aid of inductive-coupled plasma. Such etching process yielded a wavy pattern of the vertical surface with surface roughness of 0.15–0.17 μm. The main fabrication steps described above are shown schematically in Fig. 1. After these processes were completed, a pyrex-7740 glass wafer (thickness, 525 μm) having two holes as inlet and outlet ports of the liquid was anodically bonded to the back side of the silicon substrate to cover the fluid manifolds and microchannels. The width of the fabricated channel is either 50 μm or 100 μm so that the dimensions of the channel are 50 × 50, 50 × 100 and 100 × 100 with 15 mm length. The manifolds were 5 mm wide, 5 mm long, and 100 μm deep. The test chip was inserted into PCB (printed circuit board) and was connected to electrical equipments using wire ball bonding. Finally model chip was insulated thermally by using the resin epoxy and silicon rubber. A schematic of the complete device with dimensions in mm are shown in Fig. 2.

3. Experimental apparatus

A schematic of experimental apparatus is shown in Fig. 3. The apparatus consists of (a) working fluid handling system, (b)

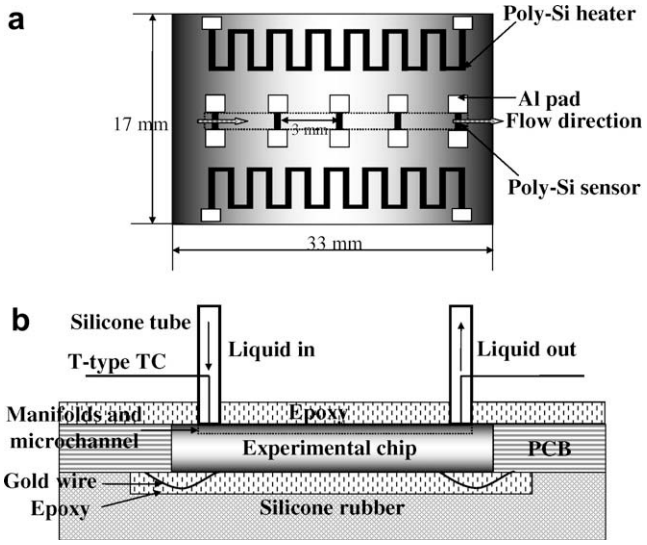

Fig. 2. Schematics of chip for convection experiment; (a) micro heaters and thermo-sensors and (b) chip setting (not to scale).

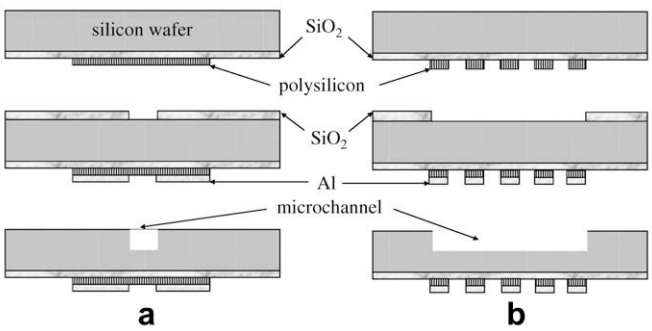

Fig. 1. Schematic of major fabrication steps; (a) end view and (b) side view.

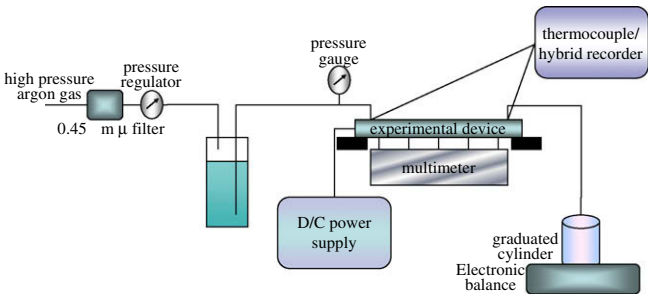

Fig. 3. Schematic of experimental apparatus.

microchannel test chip, and (c) data acquisition system. The working fluid handling system includes a high-pressure gas source, a pressurized fluid reservoir, micro filter, a pressure gauge, and a volumetric graduate. Nanofluids with suspending Al_2O_3 nanoparticles (Sigma) in base fluids were used as working fluids. The size of nanoparticles suspended in working fluids was measured by light scattering equipment (ELS-8000, Otsuka Electronic, Japan). The average size of Al_2O_3 nanoparticle is about 170 ± 10 nm.

The base fluids used were distilled water and a mixture of 50% of water and 50% of ethylene glycol. The nanofluids were prepared by ultrasonic method without using surfactant. The working fluid was driven by a high-pressure argon gas, and the driving pressure was adjusted by a pressure regulator. The liquid was freely discharged from the outlet manifold so that the outlet pressure would be atmospheric. The mass flow rate of the working fluid was measured by reading the liquid volume flowed through the graduated cylinder during 20 min and the fluid mass was measured by an electronic scale. A pressure gauge was used to monitor the fluid pressure near the inlet manifold. The power to the heater in the test chip was supplied by a DC voltage source. The voltage values from the two calibrated T-type thermocouples to measure the liquid temperatures at inlet and outlet ports, and resistance values from the polysilicon sensors to measure the wall surface temperatures along the channel were monitored by a multi meter (HP 34401A). All data at selected driving pressures to the microchannel and/or at selected powers to the heater were obtained at steady state conditions. The nanofluid at approximately 21–24 °C was fed into the input manifold through the inlet hole at driving pressures up to 0.240 MPa.

4. Experimental procedures

4.1. Sensor calibration

Although the polysilicon line heater on SiO_2 layer is a good sensor to measure the temperature [20,21], the resistance values from the sensors could change depending on the degree of phosphorus doping, the sensor dimensions fabricated and the condition of wire bonding. Thus, all the temperature sensors were calibrated before measurements. The resistance values were considerably different depending on the temperature among sensors, even though the temperature was linearly related to the resistance.

4.2. Data acquisition of heat transfer

Local fluid temperature $T_f(x)$ along the channel was obtained through the energy balance at constant heat flux condition.

$$T_f(x) = T_{in} + \frac{q''}{\dot{m}c_p}(A_{res} + P_{ch} \cdot x) \quad (1)$$

Correspondingly the local convective heat transfer coefficient and the corresponding Nusselt number along the channel were obtained from the Newton's cooling law. The estimated liquid temperatures along the channel with the measured wall temperature data along the channel and liquid temperatures at the inlet and outlet are shown in Fig. 4 for a case of $\phi = 1.8$ and $Re = 89.9$ in $50 \times 50\ \mu m^2$ microchannel.

$$h(x) = q''/(T_w(x) - T_f(x)) \quad (2)$$

$$Nu = hD_h/k_N \quad (3)$$

Thermal conductivities of the nanofluids used in this study were not measured but estimated using the theoretical correlation by Prasher et al. [12,13]. A reason for using the estimated values is that the thermal conductivities of water-based and ethylene glycol-based nanofluids with Al_2O_3 nanoparticles are well predicted by the semi-empirical method by Prasher et al. within ±10% [12,13]. Consequently, one can develop a Nusselt number correlation reasonably by using the estimated value of the thermal conductivity of nanofluids to predict the heat transfer coefficients. In fact, the relative error due to the uncertainty of the conductivity of nanofluids by the Nusselt number correlation to predict the heat transfer coefficients is approximately ±4%, which is comparable to the relative error in the heat transfer measurement, ±4.5%. The thermal conductivities of water and ethylene glycol mixture were obtained using the Filippov correlation [22]. The effective thermal conductivities of nanofluids of Al_2O_3 suspended in water or ethylene glycol turned out to increase linearly with the volume fraction of the oxide particles in the host liquids [6]. For example, the thermal conductivity of nanofluid increases 12% at the volume fraction of 1.8 % of Al_2O_3 in water. Viscosities of working fluids were measured by a viscosity meter (DV-II+ Pro, Brookfield, US).

4.3. Error analysis

The relative error in mass flow rate measurements was estimated to be approximately ±0.5%. Since the error in the measurement of channel area is less than ±0.3% and the magnitude of the mass flow rate is accurate within ±0.8%.

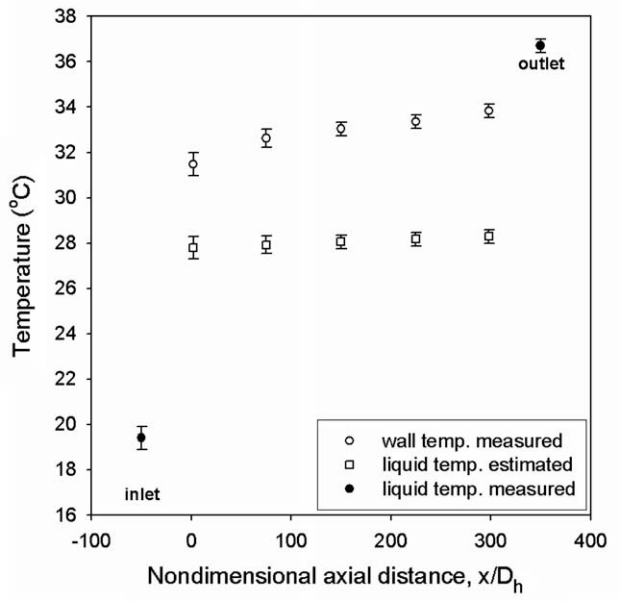

Fig. 4. Estimated liquid temperatures along the channel with measured wall temperatures and liquid temperatures at the inlet and outlet.

The heat flux given in Eq. (2) was calculated by using the following equation by assuming that uniform heat generates in the silicon wafer;

$$q'' = Q_{\text{chip}}/(A_{\text{res}} + P_{\text{ch}} \cdot L) \quad (4)$$

Q_{chip} in Eq. (4) is equal to the voltage times the current to the chip. The current to the chip was determined by measuring the voltage drop across a resistor connected with a series of chips. The error of the current measured is less than ±0.005 A so that the estimated uncertainty in the heat flux is about ±1.25% at low powers and ±1.02% at high powers with accounting for the error in the measurement of the chip surface area below ±1.0%. The error in the measurement of the wall temperature by using the polysilicon sensors is about ±0.5 °C and the error in the measurement of the liquid temperature by the T-type thermocouples is also about ±0.5 °C so that the estimated experimental errors for heat transfer coefficient are about 4.4% at the lowest heat flux and 3.9% at the highest one. The error ranges encountered in the measurement of the wall and liquid temperatures and of the heat transfer coefficients are shown the corresponding figures.

5. Results and discussions

Several particle volume fractions of 0.6%, 1.2% and 1.8% were used in this experiment. The Reynolds numbers tested are in the range between 5 and 300. Fig. 5 shows the local convective heat transfer coefficients for nanofluids with various volume fractions of nanoparticle and pure water in 50 × 50 μm² channel at Reynolds numbers of 14.0 and 80.0. Appreciable increase more than 32% in the convective heat transfer coefficient for the nanofluids with 1.8 volume percent of Al_2O_3 nanoparticle compared to the case of pure water was obtained. Similar trend in the local heat transfer coefficient was obtained for the same nanofluid in 100 × 100 μm² microchannel as shown in Fig. 6. At the Reynolds number of 80.0, the convective heat transfer coefficient in the entrance region up to $x/D_h = 50$ is significantly higher than that in the other regions, which is similar to the results obtained by Wen and Ding [18] with nanofluids in a minichannel. However no entrance region effect in the heat transfer coefficient was observed at $Re = 14.0$ in 50 × 50 μm² channel and at $Re = 60.0$ in 100 × 100 μm² channel.

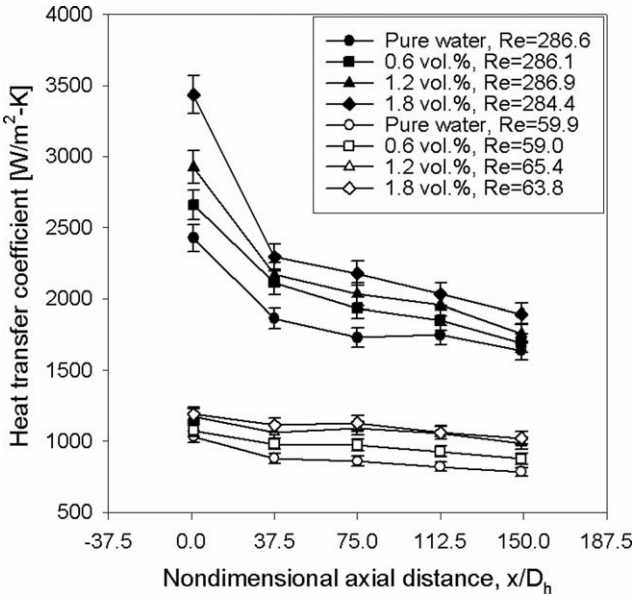

Fig. 6. Local heat transfer coefficients for nanofluids with various volume fractions of Al_2O_3 nanoparticles and distilled water in 100 × 100 μm² microchannel.

As can be seen from Figs. 5 and 6, the enhancement in the heat transfer coefficient of nanofluids becomes appreciable at higher Reynolds number. Also, the entrance regime effect becomes more pronounced at the high Reynolds number of 280, as shown in Fig. 6. The magnitude of the heat transfer coefficients obtained for the nanofluids in microchannel of 50 μm hydraulic diameter at $Re = 80$, which are about 2000–3000 W/m² K are comparable to those obtained for Cu–water nanofluids in minichannel of 4.5 mm diameter at $Re = 1000$ [18]. Fig. 7 shows the local heat transfer coefficients for nanofluids with various volume fractions of Al_2O_3 nanoparticles and water/EG mixture in 100 × 100 μm² microchannel. Fig. 7 shows the local heat transfer coefficients for nanofluids with various volume fractions of Al_2O_3 nanoparticles and water/EG mixture in 100 × 100 μm² microchannel. The viscos-

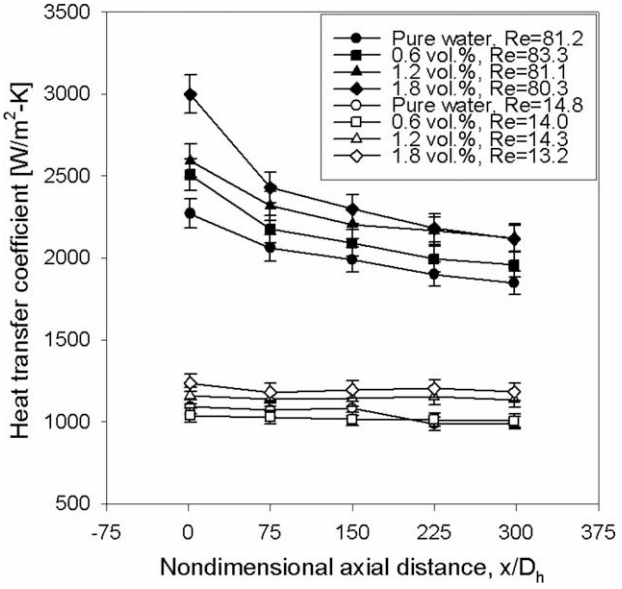

Fig. 5. Local heat transfer coefficients for nanofluids with various volume fraction of Al_2O_3 nanoparticle and distilled water in 50 × 50 μm² microchannel.

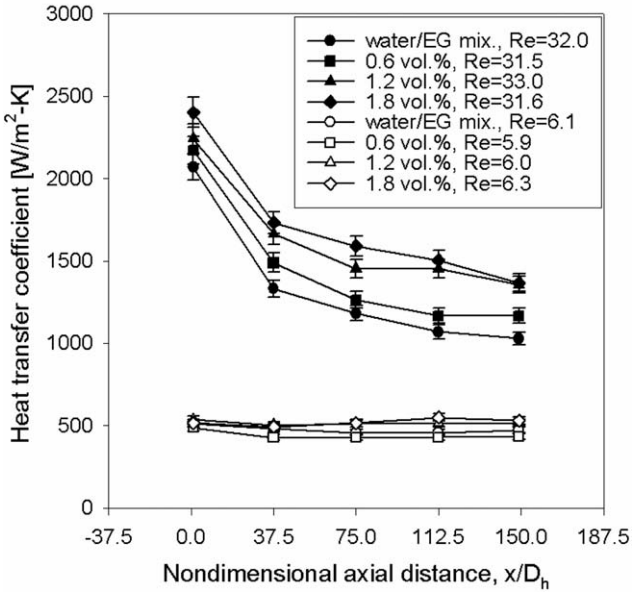

Fig. 7. Local heat transfer coefficients for nanofluids with various volume fractions of Al_2O_3 nanoparticles and water/EG mixture in 100 × 100 μm² microchannel.

ity of nanofluids based on water/EG mixture have about four times greater than those of the nanofluids based on distilled water, so the fluid velocities were very low in the microchannels. In fact, we did not obtain the stable fluid flow in the $50 \times 50\ \mu m^2$ and $50 \times 100\ \mu m^2$ microchannels. Therefore, EG based nanofluids turn out to be not suitable for working fluid in the microchannels.

Wen and Ding [23] argued that a significant non-uniformity in nanoparticle concentration inside the channel due to particle migration affected the local thermal conductivity and viscosity of the fluid, which resulted in the Nesselt number variation along the channel. They predicted that entrance effect will be more significant for larger particle. However, in our experiment where nanoparticle of larger diameter of 170 μm was used, similar entrance effect in the heat transfer coefficient was obtained compared to the Wen and Ding's results with a size range of 27–56 nm Al_2O_3 nanoparticles. Xuan and Li [17] obtained 39% increase in the Nusselt number for the nanofluid with the volume fraction of 2.0% of Cu nanoparticles in minichannel, compared with the case of water. Such remarkable increase in the Nusselt number for the Cu nanofluid in their study may be due to the turbulent flow effect.

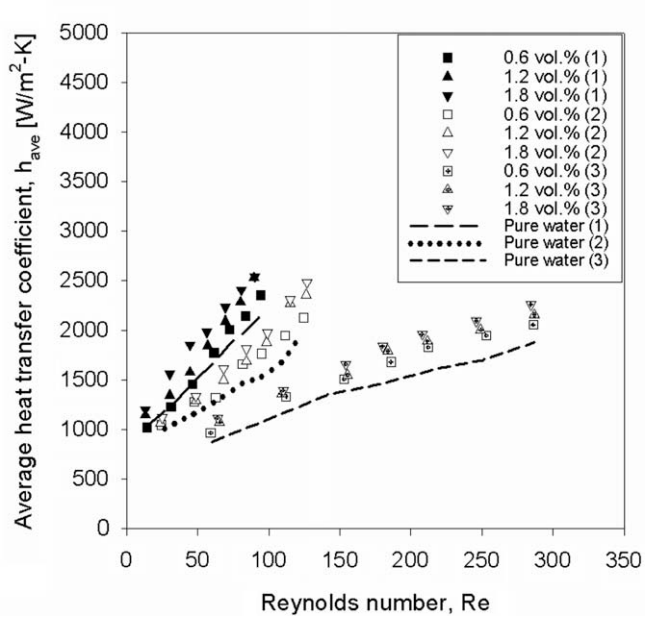

Fig. 8. Heat transfer coefficient versus Reynolds Number.

Fig. 8 shows the heat transfer coefficients versus Reynolds numbers of pure water, various nanofluids and different microchannels. The heat transfer coefficients of all nanofluids are greater than those of their base fluids (i.e. pure water). In relatively small microchannel ($50 \times 50\ \mu m^2$), the heat transfer coefficients of both nanofluids and pure water at low Reynolds numbers are comparable to or higher than those obtained at high Reynolds number in relatively large microchannels, which shows the heat transfer characteristics of microchannels.

The thermal conductivity of nanofluids depend on the species and sizes of the nanoparticles, the concentration of nanoparticles in working fluids and the combination of nanoparticles and working fluid properties [6,7]. However, at present, various correlations were proposed to predict the thermal conductivity of nanofluids [12,13,18], which reasonably provides a tool to estimate the thermal conductivity of nanofluids. The relative error in our estimation for the thermal conductivity of nanofluids is less than ± 20% so that the Nusselt number correlation proposed in this study may provide, at least, a trend for the heat transfer characteristics of nanofluids in microchannel.

Fig. 9 illustrates trends of the Nusselt number depending on the Reynolds number for the tested nanofluids with various volume

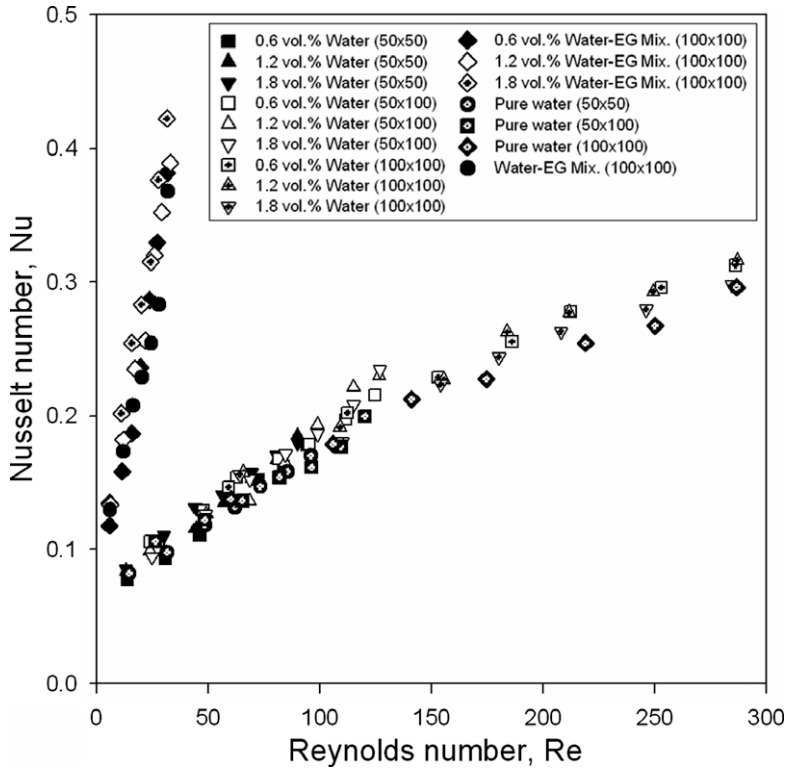

Fig. 9. Dependence of Nusselt number on Reynolds number in different dimensions of microchannels of $50 \times 50\ \mu m^2$ (1), $50 \times 100\ \mu m^2$ (2) and $100 \times 100\ \mu m^2$ (3) for the water-based and the water and ethylene glycol-based nanofluids as noted by "mix."

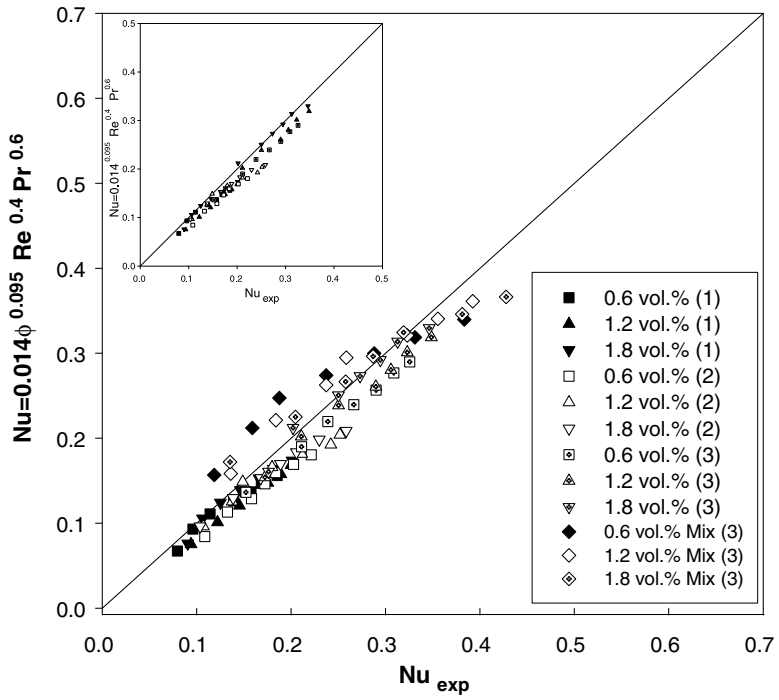

Fig. 10. Correlated Nusselt number versus measured Nusselt number. Inset shows the case of water-based nanofluids.

fractions of nanoparticles. As can be seen in this figure, two distinct lines were appeared for the nanofluids having quite different Prandtl number. However, the experimental data of the Nusselt number do not vary very much with the volume fraction of nanoparticles for the Reynolds number ranges tested. As confirmed from Figure 8, the Nusselt number obtained for nanofluids in microchannels for laminar flow regime is no longer constant [3,24] and considerably less than the theoretical value of 4.0–5.6 in microchannel [25]. Qu et al. [26] obtained nearly constant value of Nusselt number for laminar flow of water in trapezoidal silicon microchannels. They agued that the measured lower Nusselt number of 1–2 might be due to the surface roughness of the channel walls, which induced roughness viscosity. However, Qu et al.'s experimental results contradict the observed result of linear

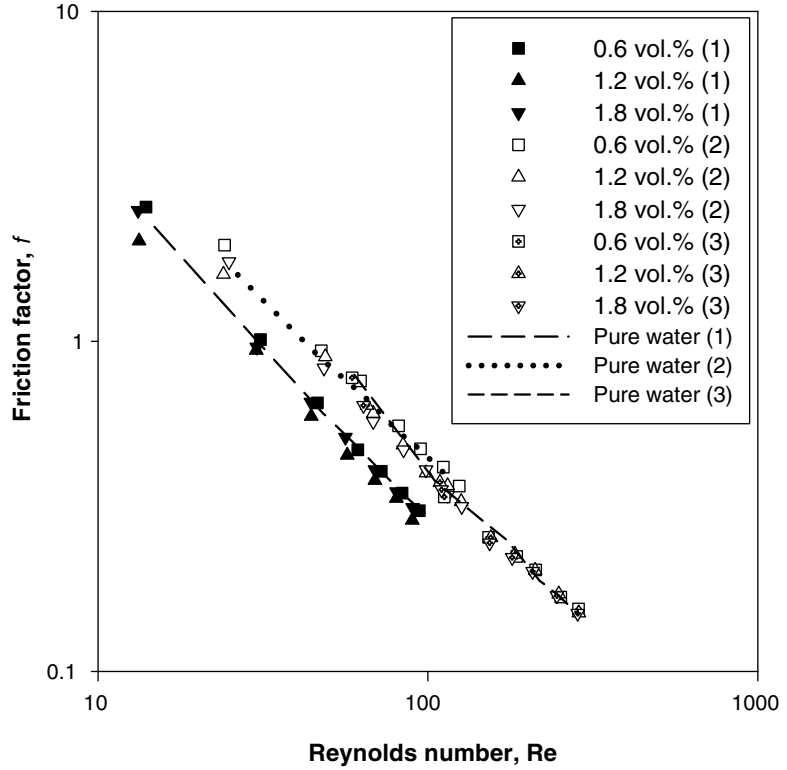

Fig. 11. Friction factors of Al_2O_3 nanofluids and distilled water in different dimension of microchannels of $50 \times 50\ \mu m^2$ (1), $50 \times 100\ \mu m^2$ (2) and $100 \times 100\ \mu m^2$ (3) for the water-based and the water and ethylene glycol-based nanofluids as noted by "mix."

dependence of Nusselt number on Reynolds number for laminar flow regime in microchannels in this study and in minichannels [17]. The Nusselt number less than 0.5 which was observed in our study indicates that the convective heat transfer in micro/nano channels does not increase linearly with the decrease in the channel size. Certainly one cannot get infinite convective heat transfer coefficient with the nanosize channel.

With slight modification of the a type of the Dittus–Boelter correlation for turbulent flow in macrochannels, the measured data of the Nusselt number for the various nanofluids of laminar flow regime in microchannels can be correlated by the following equation with considering the volume fraction of nanoparticles as shown in Fig. 10.

$$Nu = 0.014\phi^{0.095}Re^{0.4}Pr^{0.6} \quad (5)$$

The above correlation is reasonably good for the water-based nanofluids as shown in the insert of Fig. 10. Compared to the type of the Dittus-Boelter correlation for turbulent flow, the Nusselt number data for the nanofluids tested depend more strongly on the fluid properties. The fact that the Nusselt number obtained has moderate dependence on the Peclet number, $Pe = RePr$, which is quite different from the heat transfer mechanism for the laminar flow in macrochannels [26]. Similar correlation given in Eq. (5) with less dependence on the volume fraction of nanoparticles was obtained when one employed the thermal conductivity of base fluids.

Fig. 11 shows the friction factors for the nanofluids with several volume fractions of nanoparticles in different dimension of microchannels. As can be seen in this figure, the measured values of the friction factor are close to the theoretical value from the correlation for the flow in microchannels, $f = 56.9/Re_{D_h}$ [27]. Minor losses at microchannel inlet and outlet were analyzed and, consequently, could be neglected at microchannel flow of pure water [27], where the details were described. Obviously, the friction factors of the tested nanofluids are close to those of water at the same Reynolds number. Even in the smaller dimension of microchannel ($50 \times 50\ \mu m^2$), the measured friction factors decrease somewhat compared to those for the larger channel.

6. Conclusions

The convective heat transfer coefficient and the friction coefficient of nanofluids of Al_2O_3 with diameter of 170 nm in microchannels were measured. Appreciable enhancement of the convective heat transfer coefficient of the nanofluids with the base fluid of water and a mixture of water and ethylene glycol at the volume fraction of 1.8 volume percent was obtained without major friction loss. It has been found that the Nusselt number increases with increasing the Reynolds number in laminar flow regime, which is contradictory to the result from the conventional analysis.

Acknowledgements

Two (Jung-Yeul Jung and Hoo-Suk Oh) of authors have been supported by the Second Stage of BK21 program.

References

[1] D.B. Tuckerman, R.F.W. Pease, High-performance heat sinking for VLSI, IEEE Electr. Device Lett. EDL-2 (1981) 126–129.
[2] T. Kishimoto, T. Ohsaki, VLSI packaging technique using liquid-cooled channels, IEEE Trans. Compon. Hybr. CHMT-9 (1986) 328–335.
[3] B.X. Wang, X.F. Peng, Experimental investigation on forced convection heat transfer through microchannels, Int. J. Heat Mass Transfer 17 (1994) 73–82.
[4] L. Jiang, J. Mikkelson, J. Koo, D. Huber, S. Yao, L. Zhang, P. Zhou, J.G. Maveety, R. Prasher, J.G. Santiago, T.W. Kenny, K.E. Goodson, Closed-loop electroosmotic microchannel cooling system for VLSI circuits, IEEE Trans. Compon. Pack. Tech. 25 (2002) 347–355.
[5] H. Masuda, A. Ebata, K. Teramae, N. Hishinuma, Alteration of thermal conductivity and viscosity of liquid by dispersing ultra fine particles (dispersion of γ-Al_2O_3, SiO_2 and TiO_2 ultra fine particles), Netsu Bussei (Japan) 4 (1993) 227–233.
[6] S. Lee, S.U.S. Choi, S. Li, J.A. Eastman, Measuring thermal conductivity of fluid containing oxide nanoparticles, ASME J. Heat Transfer 121 (1999) 280–289.
[7] J.A. Eastman, S.U.S. Choi, S. Li, W. Yu, L.J. Thompson, Anomalously increased effective thermal conductivities of ethylene glycol-based nanofluids containing copper nanoparticles, Appl. Phys. Lett. 78 (2001) 718–720.
[8] Q.-Z. Xue, Model for effective thermal conductivity of nanofluids, Phys. Lett. A 307 (2003) 313–317.
[9] S.P. Jang, S.U.S. Choi, Role of Brownian motion in the enhanced thermal conductivity of nanofluids, Appl. Phys. Lett. 84 (2004) 4316–4318.
[10] J. Koo, C. Kleinstreuer, A new thermal conductivity model for nanofluids, J. Nanopart. Res. 6 (2004) 577–588.
[11] P. Bhattacharya, S.K. Saha, A. Yadav, P.E. Phelan, R.S. Prasher, Brownian dynamics simulation to determine the effective thermal conductivity of nanofluids, J. Appl. Phys. 95 (2004) 6492–6494.
[12] R. Prasher, P. Bhattacharya, P.E. Phelan, Thermal conductivity of nanoscale colloidal solutions (nanofluids), Phys. Rev. Lett. 94 (2005) 025901.
[13] R. Prasher, P. Bhattacharya, P.E. Phelan, Brownian-motion-based convective-conductive model for the effective thermal conductivity of nanofluids, ASME J. Heat Transfer 128 (2006) 588–595.
[14] C.H. Chon, K.D. Kihm, Thermal conductivity enhancement of nanofluids by Brownian motion, ASME J. Heat Transfer 127 (2005) 810.
[15] B.C. Pak, Y.I. Cho, Hydrodynamic and heat transfer study of dispersed fluids with submicron metallic oxide particles, Exp. Heat Transfer 11 (1998) 151–170.
[16] S. Lee, S.U.S. Choi, Applications of metallic nanoparticle suspensions in advanced cooling system, in: Y Kwon, D.C. Davis, H.H. Chung (Eds.), Recent Advances in Solid/Structures and Application of Metallic Materials, PVP-vol. 342/MD-vol. 72, ASME, New York, 1996, pp. 227–234.
[17] Y. Xuan, Q. Li, Investigation on convective heat transfer and flow features of nanofluids, ASME J. Heat Transfer 125 (2003) 151–155.
[18] D. Wen, Y. Ding, Experimental investigation into convective heat transfer of nanofluids at the entrance region under laminar flow conditions, Int. J. Heat Mass Transfer 47 (2004) 5181–5188.
[19] J. Buongiorno, Convective transport in nanofluids, ASME J. Heat Transfer 128 (2006) 240–250.
[20] J.Y. Lee, H.C. Park, J.Y. Jung, H.Y. Kwak, Bubble nucleation on micro line heaters, ASME J. Heat Transfer 125 (2003) 687–692.
[21] J.Y. Jung, J.Y. Lee, H.C. Park, H.Y. Kwak, Bubble nucleation on micro line heaters under steady or finite pulse of voltage input, Int. J. Heat Mass Transfer 46 (2003) 3897–3907.
[22] R.C. Reid, J.M. Prausnitz, B.E. Poling, The Properties of Gases & Liquids, fourth ed., McGraw-Hill, Singapore, 1986.
[23] D.S. Wen, Y. Ding, Effect of particle migration on heat transfer in suspensions of nanoparticles flowing through minichannels, Microfluids and Nanofluids 1 (2005) 183–189.
[24] H.Y. Wu, P. Cheng, An experimental study of convective heat transfer in silicon microchannels with different surface conditions, Int. J. Heat Mass Transfer 46 (2003) 2547–2556.
[25] D.B. Tuckerman, Heat-Transfer Microstructures for Integrated Circuits, Ph.D. Thesis, Stanford University, 1984.
[26] W. Qu, G.M. Mala, D. Li, Heat transfer for water flows in trapezoidal silicon microchannels, Int. J. Heat Mass Transfer 43 (2000) 3925–3936.
[27] J.Y. Jung, H.Y. Kwak, Fluid flow and heat transfer in microchannels with rectangular cross section, Heat Mass Transfer 44 (2008) 1041–1049.